Available online at www.sciencedirect.com
SCIENCE DIRECT
International Journal of Solids and Structures 43 (2006) 4323–4341
INTERNATIONAL JOURNAL OF SOLIDS and STRUCTURES
www.elsevier.com/locate/ijsolstr

Flexural-torsional buckling of misaligned axially moving beams II. Vibration and stability analysis

Kevin Orloske [a], Robert G. Parker [b,*]

[a] Ohio State University, 650 Ackerman Rd., Columbus, OH 43202, United States
[b] Department of Mechanical Engineering, Ohio State University, 650 Ackerman Rd., Columbus, OH 43202, United States

Received 8 March 2005
Available online 17 October 2005

Abstract

This paper addresses the stability and vibration characteristics of three-dimensional steady motions (equilibrium configurations) of translating beams undergoing boundary misalignment. System modeling and equilibrium solutions for bending in two planes, torsion, and extension were presented in Part I of the present work. Stability is determined by linearizing the equations of motion about a steady motion and calculating the eigenvalues using a finite difference discretization. For the case of no misalignment, the calculated eigenvalues are compared to known values. When the beam is misaligned, the system initially enters a planar configuration and the results indicate that the planar equilibria lose stability after the first bifurcation point. Eigenvalue behavior of the planar equilibria after the first bifurcation point is shown to be strongly influenced by translation speed. Eigenvalue behavior about non-planar equilibria and vibration modes about selected equilibria are also presented.

Keywords: Axially moving; Beam; Vibration; Stability; Flexural-torsional; Buckling

1. Introduction

In Part I of the present work (Orloske et al., 2005), the equations of motion of a three-dimensional axially moving beam under tension were developed, and the equilibrium equations of the system were analyzed using continuation and bifurcation software (Doedel et al., 1997). Planar and three-dimensional non-planar steady motions (or equilibria) both occur. In order to understand what misalignments cause buckling and into which buckled configuration the system will deform, the stability of the equilibria must be analyzed.

In this paper, stability and free vibration characteristics are determined by linearizing the equations of motion about a general three-dimensional equilibrium configuration and calculating the eigensolutions using

* Corresponding author. Tel.: +1 614 688 3922; fax: +1 614 292 3163.
E-mail address: parker.242@osu.edu (R.G. Parker).

0020-7683/$ - see front matter © 2005 Elsevier Ltd. All rights reserved.
doi:10.1016/j.ijsolstr.2005.08.015

a finite difference discretization. For purposes of comparison, the eigensolutions about the trivial configuration are determined first. Then, eigensolutions about selected non-trivial equilibria are analyzed. Attention focuses on how the eigensolutions and equilibrium stability evolve as the equilibria change due to misalignment and changing translation speed. Frequent reference will be made to the equilibria in Part I of the present work.

Previous work on the free vibration characteristics of translating beams is limited to single-plane flexural (Mote, 1965; Simpson, 1973) or coupled flexural–extensional (Wickert, 1992) systems. Wickert examined the free vibration characteristics of a coupled flexural–extensional translating beam under tension. He included the effect of translation speed on the fundamental frequency and the influence of nonlinear stiffness terms on the free response. A stability and bifurcation analysis of the same system was conducted in (Pellicano and Vestroni, 2000). Hwang and Perkins (1992) investigated the vibration characteristics of a translating beam that includes the effect of initial curvature due to the bending moment created by the bounding pulleys. Their work highlights the sensitivity of the critical speed behavior in the presence of system imperfections.

2. Eigenvalue problem formulation

To assess the behavior of the system for small motions about an equilibrium, the equations of motion derived in (Orloske et al., 2005) are linearized about an arbitrary equilibrium configuration. These equations are

$$\begin{aligned} &\breve{G}'_{\alpha} = \ddot{\alpha} + \dot{\alpha}' c, \quad \alpha = u, v, w \\ &\breve{G}_{\theta} = 0 \end{aligned} \tag{1}$$

where expressions for the $\breve{G}_{\alpha}$ are given in the Appendix and all notation follows (Orloske et al., 2005).

Let the deformation variables be collected in the vector

$$\mathbf{Y}^* = \begin{bmatrix} u(x,t) \\ v(x,t) \\ w(x,t) \\ \theta(x,t) \end{bmatrix} \tag{2}$$

By assuming the separable solution

$$\mathbf{Y}^*(x,t) = \mathbf{Y}(x)\mathrm{e}^{\lambda t} \tag{3}$$

the following quadratic eigenvalue problem is formed

$$(\lambda^2 \mathbf{M} + \lambda \mathbf{G} + \mathbf{K})\mathbf{Y} = 0 \tag{4}$$

where **M**, **G**, and **K** are spatial mass, gyroscopic, and stiffness operators constructed from (1). The stability of the system is assessed from the eigenvalues of (4). Due to the cumbersome length of the linearized equations of motion, the symmetry and definiteness properties of **M**, **G**, and **K** are not verified. It is anticipated, and subsequently verified, that the system possesses the properties of a conservative, gyroscopic continuum, including complex eigensolutions that always occur in complex conjugate pairs. Divergence and flutter instabilities occur at high speed.

The natural frequencies and vibration modes about a specified equilibrium are determined by finite difference discretization of (4). The beam is discretized into $n-1$ sections of uniform width h. Spatial derivatives in the four equations of motion are approximated using the central difference expressions (Koenig, 1998)

$$\begin{aligned} &\left.\frac{\mathrm{d}Y}{\mathrm{d}x}\right|_i = \frac{1}{2h}(-Y_{i-1} + Y_{i+1}), \quad \left.\frac{\mathrm{d}^3Y}{\mathrm{d}x^3}\right|_i = \frac{1}{2h^3}(-Y_{i-2} + 2Y_{i-1} - 2Y_{i+1} + Y_{i+2}) \\ &\left.\frac{\mathrm{d}^2Y}{\mathrm{d}x^2}\right|_i = \frac{1}{h^2}(Y_{i-1} - 2Y_i + Y_{i+1}), \quad \left.\frac{\mathrm{d}^4Y}{\mathrm{d}x^4}\right|_i = \frac{1}{h^4}(Y_{i-2} - 4Y_{i-1} + 6Y_i - 4Y_{i+1} + Y_{i+2}) \end{aligned} \tag{5}$$

where Y_i is a deformation variable (one of u, v, w, θ) evaluated at mesh point i. Let mesh points 1 and n reside on the domain boundary. When (4) is expressed at each interior mesh point, $4n-8$ equations are obtained from four equations at each of $n-2$ mesh points. u and θ are acted on by second-order spatial derivatives

in (4), so, from (5), these variables must be evaluated at mesh points 1 and n. The necessary values are supplied by the boundary conditions. v and w, however, are acted on by third and fourth-order operators and, from (5) at points 2 and $n-1$, must be evaluated beyond the domain boundaries at points 0 and $n+1$, in addition to points 1 and n. By using the zero slope boundary conditions with the first of (5) the following relations are obtained for v and w at the points 0 and $n+1$

$$Y_0 = Y_2, \quad Y_{n+1} = Y_{n-1} \tag{6}$$

Given the length of the linearized equations, the finite difference process is automated with computer algebra software.

Without applying boundary conditions, the discretized forms of $\mathbf{M}$, $\mathbf{G}$, and $\mathbf{K}$ are $(4n-8)\times(4n+4)$ matrices and $\mathbf{Y}$ is a vector of dimension $4n+4$. The 12 boundary conditions are applied by defining the constraint matrix $\mathbf{D}$ such that

$$\mathbf{Y} = \mathbf{D}\widehat{\mathbf{Y}} \tag{7}$$

where $\widehat{\mathbf{Y}}$ is the vector of deformation variables at the interior mesh points and is of dimension $4n-8$. Using (7) the discretized form of the eigenvalue problem becomes

$$(\lambda^2\widehat{\mathbf{M}} + \lambda\widehat{\mathbf{G}} + \widehat{\mathbf{K}})\widehat{\mathbf{Y}} = 0 \tag{8}$$

$$\widehat{\mathbf{M}} = \mathbf{M}\mathbf{D}, \quad \widehat{\mathbf{G}} = \mathbf{G}\mathbf{D}, \quad \widehat{\mathbf{K}} = \mathbf{K}\mathbf{D} \tag{9}$$

$\widehat{\mathbf{M}}$, $\widehat{\mathbf{G}}$, and $\widehat{\mathbf{K}}$ are all square $(4n-8)\times(4n-8)$ matrices. None are symmetric or skew-symmetric due to elements arising from the boundary conditions.

The preceding finite difference formulation is for a mesh of uniform width. The numerical equilibrium solution obtained in Part I of the present work (Orloske et al., 2005) uses mesh adaptation resulting in equilibrium solutions on a non-uniform mesh of 2001 mesh points. These are linearly interpolated to a uniform mesh of n points prior to applying the finite difference method.

3. Analysis about the trivial equilibrium

The linearized equations of motion about the trivial equilibrium, which are all decoupled, are

$$\left(c^2 - \frac{1}{\mu}\right)u'' + 2c\dot{u}' + \ddot{u} = 0 \tag{10}$$

$$(\beta_\zeta - j_\zeta c^2)v^{\mathrm{IV}} + (c^2-1)v'' + 2c\dot{v}' - j_\zeta\ddot{v}'' - 2j_\zeta c\dot{v}''' + \ddot{v} = 0 \tag{11}$$

$$\left(\frac{\beta_\zeta}{\beta_\eta} - j_\eta c^2\right)w^{\mathrm{IV}} + (c^2-1)w'' + 2c\dot{w}' - j_\eta\ddot{w}'' - 2j_\eta c\dot{w}''' + \ddot{w} = 0 \tag{12}$$

$$\left[j_\xi c^2 - \mu\left(\beta_\zeta + \frac{\beta_\zeta}{\beta_\eta}\right) - \beta_\xi\right]\theta'' + 2j_\xi c\dot{\theta}' + j_\xi\ddot{\theta} = 0 \tag{13}$$

The natural frequencies are determined in closed-form for the second-order equations and by Galerkin's method for the fourth-order equations. This serves as a check for the finite difference formulation. In addition, the critical speed eigenvalue problem of these equations is obtained in closed-form and complements the associated results in Fig. 7 of (Orloske et al., 2005). All results are for the same parameters used in Table 1 of (Orloske et al., 2005) unless otherwise specified.

3.1. Natural frequencies

Eqs. (10) and (13) admit closed-form solutions of their corresponding eigenvalue problems. Letting y be u or θ, the solution $y(x,t) \to y(x)\mathrm{e}^{\mathrm{i}\omega t}$ gives the differential eigenvalue problem of (10) or (13)

$$c_1 y'' + c_2 y'\omega\mathrm{i} - c_3 y\omega^2 = 0 \tag{14}$$

where the c_i are parameters. The characteristic equation of (14) with the boundary conditions $y(0) = y(1) = 0$ is

$$\exp(\mathrm{i}\beta\omega) = \pm 1, \quad \beta = \frac{\sqrt{c_2^2 - 4c_1c_3}}{2c_1} \tag{15}$$

The parameters of (10) and (13) are such that $c_2^2 - 4c_1c_3 > 0$ and β is real for both systems. The union of solutions for $+1$ and -1 in (15) yields

$$\omega = \frac{q\pi}{\beta}, \quad q = \pm 1, 2, \ldots \tag{16}$$

With parameter values from Table 1 of (Orloske et al., 2005), the first natural frequency of (10) is 58.323, and the first natural frequency of (13) is 5.5906.

Eqs. (11) and (12), which have identical structure and differ only in their coefficients, are more complex, and their eigenvalue problem does not admit a simple closed-form solution. The first several eigenvalues of these equations are determined using a Galerkin discretization. Ten trial functions $p_i(x)$ satisfying all boundary conditions are drawn from a complete set of polynomials. Trial functions of increasing polynomial order are constructed by considering the boundary conditions and the orthonormality relation $\langle p_i, p_j \rangle = \delta_{ij}$, where δ_{ij} is the Kronecker delta and the inner product is defined as $\langle p_i, p_j \rangle = \int_0^1 p_i p_j \, \mathrm{d}x$. Using the parameters in Table 1 of (Orloske et al., 2005), the first natural frequency of (11) is 3.1496 and the first natural frequency of (12) is 27.274.

Using the exact solution to (10) and (13) along with the Galerkin solution to (11) and (12), a convergence study was performed to establish the necessary finite difference mesh resolution for the solution. The results are given in Fig. 1 and Table 1. In this work $n = 401$ mesh points are used.

3.2. Critical speeds

When the misalignment is zero and the speed is sufficiently high, a pair of complex conjugate imaginary eigenvalues approach and coalesce at zero. Above this speed instability is possible. The speeds at which these eigenvalues become zero are termed the critical speeds for zero misalignment. Such speeds were illustrated in Fig. 7 of (Orloske et al., 2005) where the critical misalignment loci touch the abscissa. In this paper, those previously determined critical speeds are shown to correspond to the critical speed eigenvalue problems of (11) and (12).

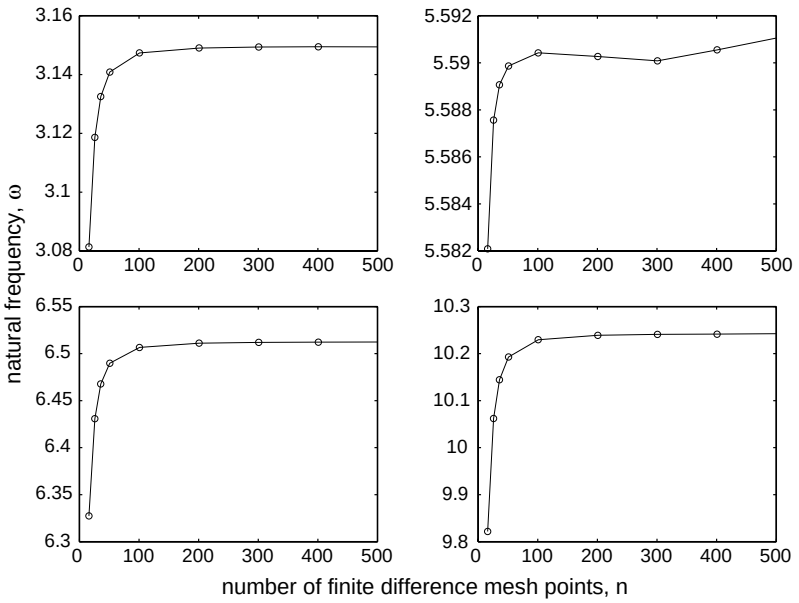

Fig. 1. Convergence study of the first four natural frequencies about the trivial equilibrium for varying numbers of finite difference mesh points.

Table 1
The first four natural frequencies about the trivial equilibrium for parameters in Table 1 of (Orloske et al., 2005)

Finite difference, $n = 401$	Analytical	Galerkin	Mode type
3.14949	N/A	3.14963	Flexural (v-dir.)
5.59055	5.59064	N/A	Torsional
6.51219	N/A	6.51257	Flexural (v-dir.)
10.24155	N/A	10.24238	Flexural (v-dir.)

Results calculated using finite difference discretization with 401 mesh points are compared to analytical (from (16)) and Galerkin results.

Table 2
The first five critical speeds about the trivial equilibrium calculated from AUTO97 (as shown in Fig. 7 of (Orloske et al., 2005)), by determining the roots of (19), and using Galerkin discretization with ten polynomial trial functions

Galerkin	AUTO97	Analytical
1.028797	1.028797	1.028797
1.058030	1.058030	1.058030
1.110482	1.110482	1.110482
1.162734	1.162732	1.162732
1.234769	1.233969	1.233969

Eqs. (10) and (13) do not yield any critical speeds for zero misalignment. For both cases, (14) with $\omega = 0$ yields

$$(c_4 c^2 - c_5) y'' = 0 \tag{17}$$

where c_4 and c_5 are constants from (10) and (13). Treating (17) as an eigenvalue problem for c^2, the only eigenvalue is $c^2 = c_5/c_4$. This eigenvalue has infinite multiplicity and implies any comparison function satisfies (10) or (13) and so is an eigenfunction. This degenerate case does not manifest itself as a critical speed in the numerical solution.

Consequently, all critical speeds for zero misalignment result from (11) and (12). These critical speed ($\omega = 0$) eigenvalue problems admit closed-form solutions. Letting y be v or w, the eigenvalue problem of (11) or (12) takes the form

$$(c_6 - c_7 c^2) y^{\mathrm{IV}} + (c^2 - 1) y'' = 0 \tag{18}$$

where c^2 is the eigenvalue. Using $y(0) = y(1) = y'(0) = y'(1) = 0$ with the general solution of (18) gives the characteristic equation

$$\sin\left(\frac{\sqrt{c^2-1}}{\sqrt{c_6 - c_7 c^2}}\right)\sqrt{c^2-1} + 2\sqrt{c_6 - c_7 c^2}\left[\cos\left(\frac{\sqrt{c^2-1}}{\sqrt{c_6 - c_7 c^2}}\right) - 1\right] = 0 \tag{19}$$

By inspection of (19) $c^2 = 1$ is a solution. When $c^2 = 1$ is substituted into (18), however, the second-order derivative term vanishes, and solution of the resulting equation under clamped–clamped boundary conditions yields the trivial solution. Therefore $c = 1$ is not a critical speed for zero misalignment.

Table 2 compares the critical speeds for zero misalignment calculated from (19) with the numerical results calculated in (Orloske et al., 2005). Results calculated using Galerkin's method are also included to demonstrate the accuracy provided by 10 polynomial trial functions. The results in Table 2 show excellent agreement between the three methods. The lowest critical speeds arise from (11). The first critical speed to arise from (12) is $c = 7.4844$.

4. Results

4.1. Eigenvalues about planar equilibria

For speeds less than $c = 1.0288$ the trivial solution is the only equilibrium, and it is stable. As discussed in (Orloske et al., 2005), when the system undergoes misalignment the initial equilibria are planar. Prior to the

first critical misalignment, the planar equilibria are the only equilibria, and these are stable. This is summarized in Fig. 7 of (Orloske et al., 2005). As the beam is misaligned further, the natural frequencies about the planar equilibria decrease until the fundamental frequency reaches zero. At this first critical misalignment, a divergence instability occurs and planar equilibria are no longer stable.

Fig. 2 illustrates how the eigenvalues change as misalignment is increased for the case of zero translation speed. Sections a, b, c, and d correspond to the first four critical misalignments. The locations of the critical misalignments agree with Fig. 7 of (Orloske et al., 2005). At each critical misalignment, a pair of purely

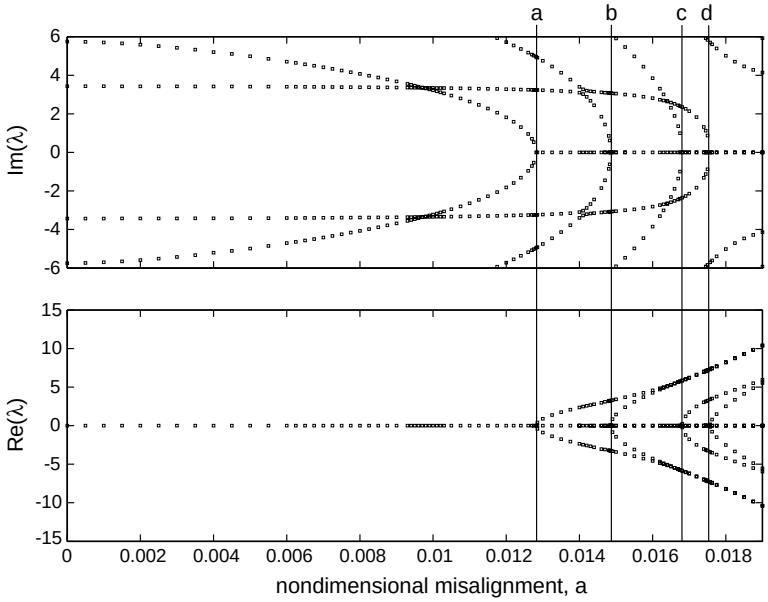

Fig. 2. Eigenvalues about the planar equilibria when $c = 0$.

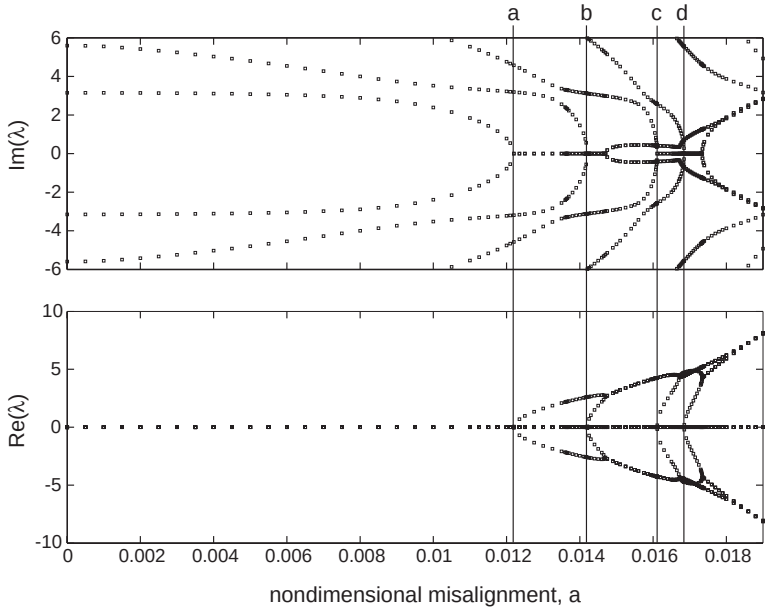

Fig. 3. Eigenvalues about the planar equilibria when $c = 0.3$.

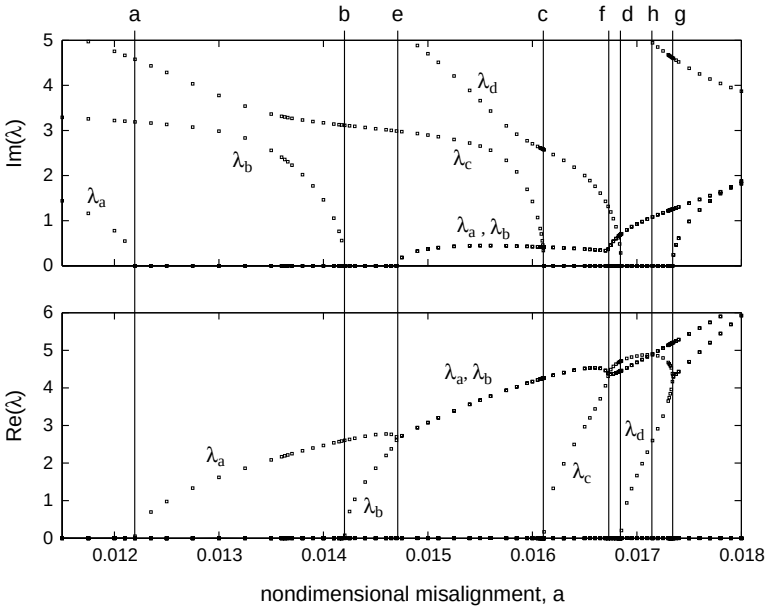

Fig. 4. Details of Fig. 3.

imaginary, complex conjugate eigenvalues coalesce and a divergence instability develops. These instabilities are terminal in that the planar equilibrium eigenvalues never regain stability as misalignment increases further.

When the translation speed is non-zero, the eigenvalue behavior is more complex. The results when $c = 0.3$ are given in Figs. 3 and 4. Again, sections a, b, c, and d correspond to the first four critical misalignments. The eigenvalue behavior near critical misalignments is the same as the zero speed case in that a pair of purely imaginary, complex conjugate eigenvalues coalesce at zero and a divergence instability develops. In contrast to the zero speed case, however, non-zero translation speed causes complex eigenvalues and flutter instabilities (eigenvalues with positive real part and non-zero imaginary part) in planar equilibria. For the purposes of discussion, let the two eigenvalues that coalesce and then form a divergence instability at section α be denoted λ_α, where $\alpha = a, b, c, d$.

At a speed of $c = 0.3$ the creation and behavior of flutter instabilities is linked to the first interaction of $\mathrm{Re}(\lambda_\alpha)$ with the real parts of other eigenvalues. At section e of Fig. 4, λ_a coalesces with λ_b and the first flutter instability develops. This occurs where $\mathrm{Re}(\lambda_b)$ first meets the real part of another eigenvalue, namely $\mathrm{Re}(\lambda_a)$. Immediately before coalescing at section e, λ_a and λ_b are purely real and hence divergent unstable. After section e, the eigenvalues separate, one acquires a positive and the other a negative imaginary part. Thus, an eigenvalue with flutter instability bifurcates from the colliding divergent eigenvalues. We label this pair λ_a, λ_b on Fig. 4. This differs from the more conventional behavior whereby flutter instability evolves from collision of two purely imaginary eigenvalues.

The first interaction λ_c has with the real part of another eigenvalue is at section f. At this section λ_c intersects the real part of the flutter instability eigenvalue pair λ_a, λ_b. This causes a sudden change in how the flutter instability eigenvalue pair λ_a, λ_b evolves with misalignment. The second time λ_c crosses a pair of flutter instability eigenvalue (section h) appears to have no impact on the eigenvalue behavior. As misalignment is increased, λ_c decreases while λ_d increases. At section g these two real eigenvalues coalesce and a new flutter instability is formed, akin to the behavior of λ_a and λ_b.

Increasing the translation speed to $c = 0.9$ changes the eigenvalue behavior dramatically. The results are given in Figs. 5 and 6. Once again, sections a, b, c, and d correspond to the first four critical misalignments. The eigenvalue behavior near the first critical misalignment is the same as the previous cases in that a pair of purely imaginary, complex conjugate eigenvalues coalesce at zero and a divergence instability develops. When misalignment is increased past the first critical misalignment, however, the eigenvalue behavior bears little resemblance to the lower speed results.

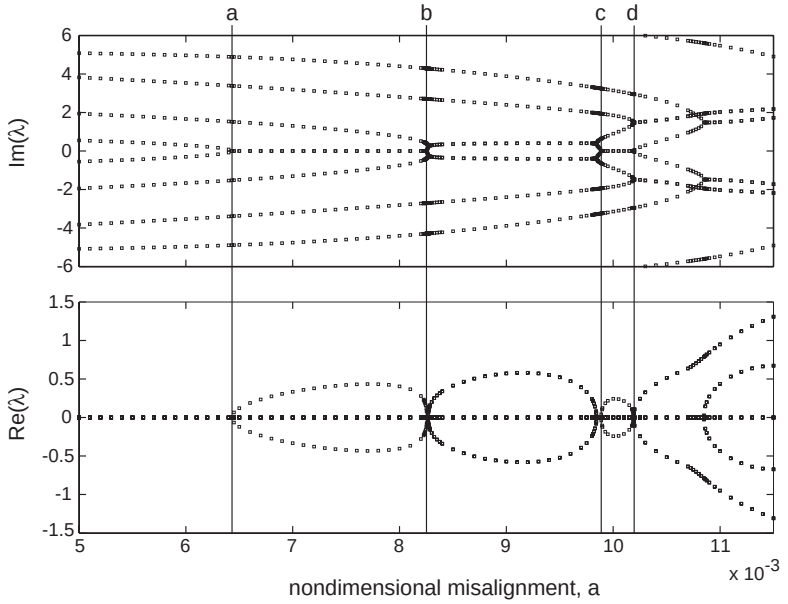

Fig. 5. Eigenvalues about the planar equilibria when $c = 0.9$.

After section a, Re(λ_a) reaches zero again at section b, at which point λ_a again becomes stable (Fig. 6a). Just after λ_a becomes stable at section b, it coalesces with λ_b at section n and flutter instability forms (Fig. 6a). This flutter instability develops in a conventional way from two colliding, purely imaginary eigenvalues, in constrast to section e of Fig. 4. For the narrow range of misalignments between sections b and n the planar equilibria regain stability (Fig. 6a). This unexpected phenomenon was not observed in the lower speed results: additional misalignment can stabilize an equilibrium that is unstable for lower misalignment. When misalignment is increased further beyond section n, Re(λ_a, λ_b) vanish at section k (Fig. 6b). At this misalignment λ_a and λ_b separate from one another as purely imaginary stable eigenvalues in a 'reverse flutter' bifurcation. One eigenvalue's imaginary part increases (let this be λ_a) while the other decreases. Im(λ_b) reaches zero at section c where the pair of purely imaginary, complex conjugate eigenvalues coalesce and a divergence instability develops. For the range of misalignments between sections k and c the planar equilibria regain stability for the second time after the first critical misalignment.

When misalignment is increased beyond the third critical misalignment (section c in Fig. 6b) λ_a coalesces with λ_d at section d and a flutter instability develops. This is a different flutter interaction than at the lower speed $c = 0.3$ (sections e and g of Fig. 4), although it resembles the λ_a, λ_b interaction at section n. For the range of misalignments after section d explored in this work, the eigenvalue pair λ_a and λ_d continue to exhibit flutter. Also at section d, Re(λ_b) reaches zero and λ_b becomes purely imaginary. From their separation at section k, λ_a had remained stable while λ_b had digressed to instability (section c). At the same point (section d), they now exchange stability through seemingly unrelated interactions: λ_a experiences flutter with λ_d while λ_b reverts from divergence to stability. At section m, Im(λ_j) intersects Im(λ_a, λ_d), but no apparent impact on eigenvalue behavior is observed. At section j, λ_j coalesces with λ_b and a new flutter instability develops, akin to the behavior of λ_a and λ_d.

The evolution of natural frequencies (Im(λ)) with misalignment is illustrated in Fig. 7 for the stationary and moving beams. When the beam is stationary, the natural frequencies experience crossing with other natural frequencies as misalignment is increased. Increasing speed to $c = 0.3$ causes the natural frequencies to untangle from one another such that the crossing of natural frequencies is replaced by curve veering. Note that for zero and non-zero speeds the natural frequencies do not decrease monotonically as misalignment is increased. Under certain ranges of misalignment some natural frequencies increase before ultimately decreasing to zero at a critical misalignment.

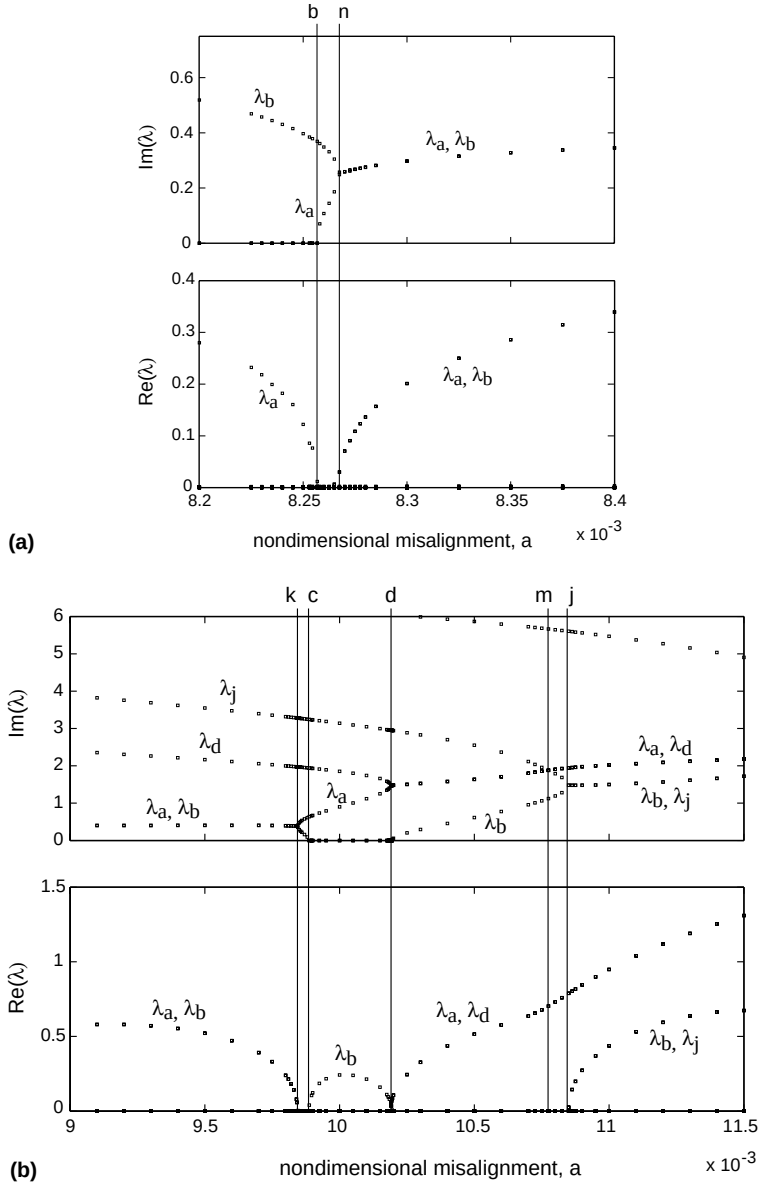

Fig. 6. Details of Fig. 5.

4.2. Eigenvalues about non-planar equilibria

At each critical misalignment an out-of-plane equilibrium bifurcates from the planar solution. Selected bifurcation branches and the first three out-of-plane solutions for $c = 0.3$ were given in (Orloske et al., 2005). The eigenvalues along the first out-of-plane solution branch starting at $a = 0.0122$ for $c = 0.3$ (see Fig. 9 of (Orloske et al., 2005)) are illustrated in Fig. 8 and indicate that this configuration is stable. $\|\theta\| = 0$ in Fig. 8 corresponds to the planar solution eigenvalues at section a of Fig. 4. Note that a smooth transition of the eigenvalues from the planar solution to the out-of-plane solution occurs as misalignment is increased.

Fig. 9 displays the eigenvalues along the second out-of-plane solution branch starting at $a = 0.0142$ for $c = 0.3$, where $\|\theta\| = 0$ in Fig. 9 corresponds to the planar solution eigenvalues at section b of Fig. 4. Again, the eigenvalues undergo a smooth transition from the planar solution to the out-of-plane solution

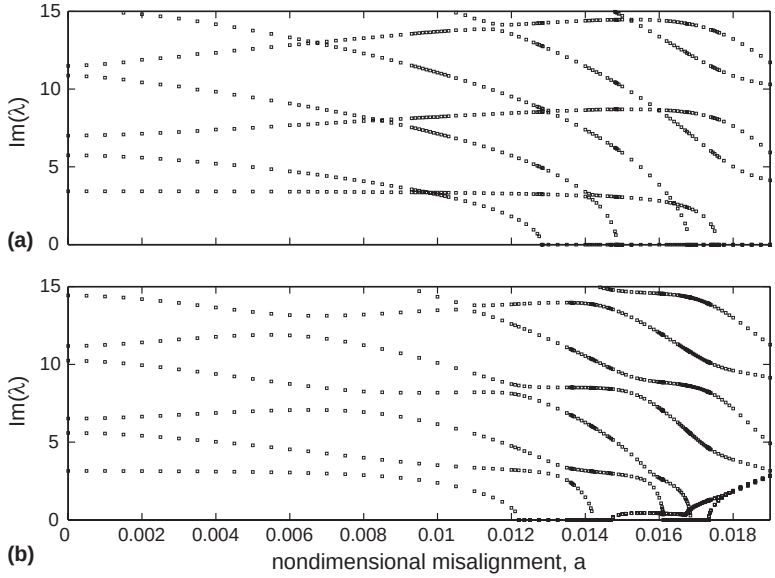

Fig. 7. (a) Imaginary part of the eigenvalues when $c = 0$. (b) Imaginary part of the eigenvalues when $c = 0.3$. Note that the real parts are not shown.

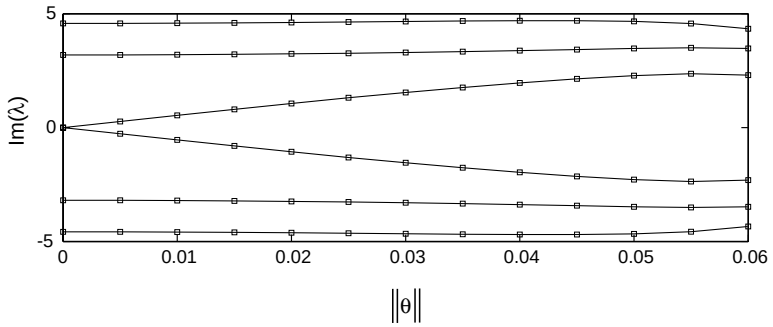

Fig. 8. Eigenvalues about the first out-of-plane solution branch in Fig. 9 of (Orloske et al., 2005) when $c = 0.3$. The real parts of all eigenvalues are zero.

as misalignment is increased. As a consequence, the divergence instability from λ_a that is present for the planar configuration in $0.0122 < a < 0.0142$ (Fig. 4) persists when one moves along the second out-of-plane solution branch. Similar trends are observed in Fig. 10 showing the eigenvalues along the third out-of-plane solution branch starting at $a = 0.0161$ for $c = 0.3$. Thus, these bifurcated out-of-plane equilibria are unstable.

For a speed of $c = 0.3$, at each critical misalignment a pair of purely imaginary, complex conjugate eigenvalues coalesce at $\lambda = 0$, and a divergence instability develops in the planar solution (Fig. 3). When buckling into an out-of-plane solution occurs, the coalescing eigenvalues at $\lambda = 0$ of the planar solution become real and unstable; in contrast, the corresponding pair of eigenvalues of the bifurcated out-of-plane solution evolve from $\lambda = 0$ to become purely imaginary and stable. In other words, buckling into an out-of-plane solution 'salvages' stability of the eigenvalues coalescing at $\lambda = 0$ for a critical misalignment. Eigenvalues other than those coalescing at $\lambda = 0$ are qualitatively unaffected by buckling. After the first critical misalignment for $c = 0.3$, the planar solution always suffers from divergence and, possibly, flutter instabilities. Because the eigenvalues change continuously along branches bifurcating into out-of-plane configurations, the first out-of-plane equilibrium branch is the only stable out-of-plane solution for the misalignments explored. Other branches inherit at least one unstable eigenvalue of the planar solution (Figs. 9 and 10).

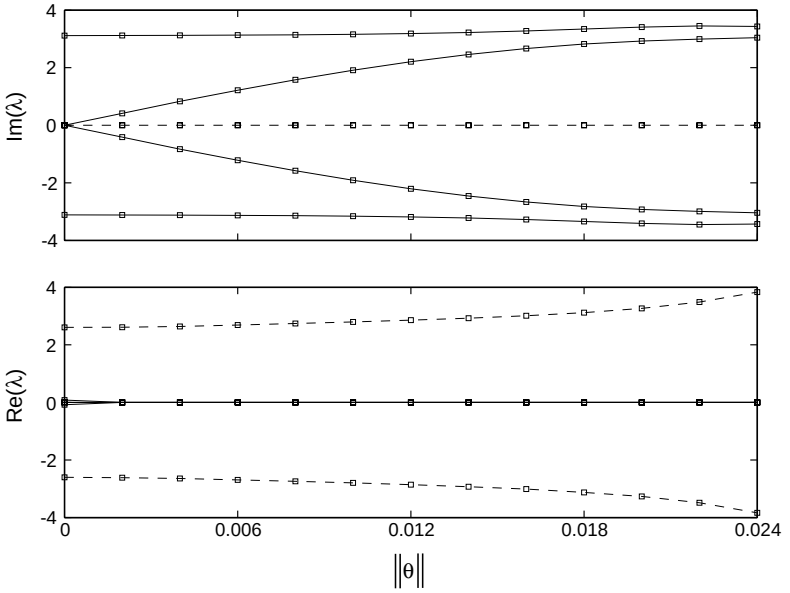

Fig. 9. Eigenvalues about the second out-of-plane solution branch in Fig. 9 of (Orloske et al., 2005) when $c = 0.3$. The dashed lines correspond to eigenvalues that cause instability.

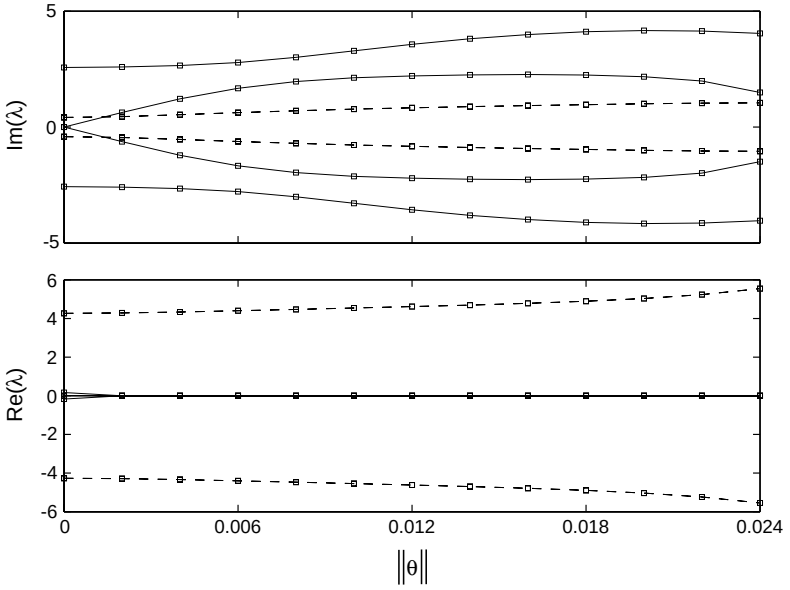

Fig. 10. Eigenvalues about the third out-of-plane solution branch in Fig. 9 of (Orloske et al., 2005) when $c = 0.3$. The dashed lines correspond to eigenvalues that cause instability.

When speed is increased to $c = 0.9$ the smooth transition of the eigenvalues from the planar solution to the out-of-plane solution remains. The eigenvalues along the first out-of-plane solution branch starting at $a = 0.00643$ for $c = 0.9$ are qualitatively identical to Fig. 8 and indicate that this configuration is stable.

Fig. 11 displays the eigenvalues along the second out-of-plane solution branch starting at $a = 0.008257$ for $c = 0.9$. $\|\theta\| = 0$ in Fig. 11 corresponds to the planar solution eigenvalues at section b of Fig. 6a. By buckling

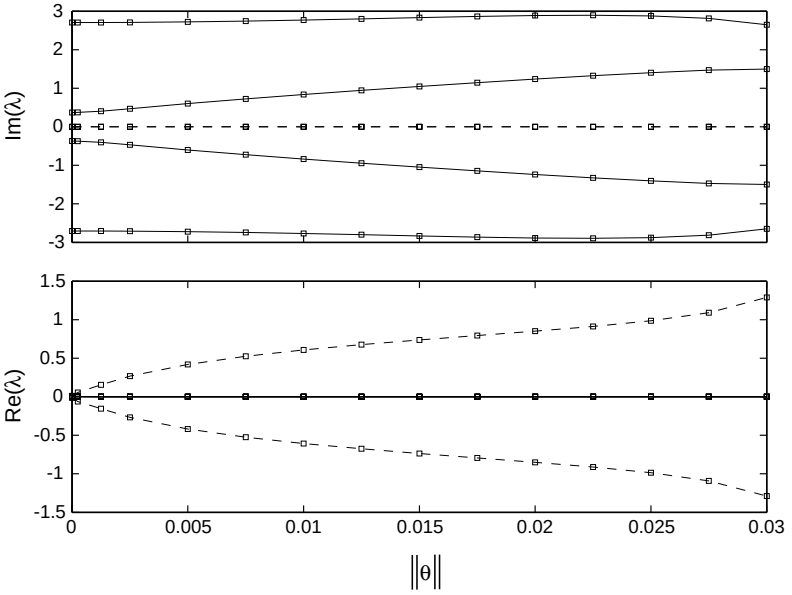

Fig. 11. Eigenvalues about the second out-of-plane solution branch in Fig. 9 of (Orloske et al., 2005) when $c = 0.9$. The dashed lines correspond to eigenvalues that cause instability.

into an out-of-plane solution at the second critical misalignment, λ_a, which is stable beyond b for the planar solution, reverts to divergence instability. Thus, this solution is unstable for all misalignments considered.

For a speed of $c = 0.9$, the planar and out-of-plane eigenvalue behavior at the first two critical misalignments show a noteworthy duality. As the first critical misalignment is crossed, the coalescing imaginary (stable) planar eigenvalues become real (unstable) in the planar solution (Fig. 5). The corresponding zero eigenvalues of the bifurcated out-of-plane solution, however, adopt the stability characteristics of the coalescing eigenvalues of the planar solution (i.e., imaginary). Converse behavior occurs at the second critical misalignment at b. The coalescing planar eigenvalues at b are real, and they regain stability beyond b. Simultaneously, the zero eigenvalues of the bifurcated out-of-plane solution become real for any misalignment greater than b (Fig. 11). The planar solution eigenvalue behavior near these first two critical misalignments is reminiscent of the eigenvalues and divergence instability of an aligned axially moving beam as speed is varied near the first two critical speeds (Wickert and Mote, 1990).

Recall that just prior to the third critical misalignment for $c = 0.9$ the planar solution regains stability (section k of Fig. 6). Consequently, at section c in Fig. 6 there are no unstable eigenvalues. The eigenvalues along the third out-of-plane solution branch starting at $a = 0.00989$ for $c = 0.9$ are illustrated in Fig. 12, where $\|\theta\| = 0$ corresponds to the planar solution eigenvalues at section c of Fig. 6. Initially this out-of-plane configuration is stable. In contrast, at lower speed ($c = 0$ and $c = 0.3$) only the first bifurcated out-of-plane solution is stable. As misalignment is increased, however, the two dashed line eigenvalue loci in Fig. 12 coalesce near $\|\theta\| = 0.0025$ and flutter instability develops.

The effect of changing translation speed on the equilibria after entering an out-of-plane solution was examined previously in Fig. 15 of (Orloske et al., 2005). For larger speeds, these solutions suffer from singularities that prevented further extension of the branches. Solutions that start from $c = 0.9$, however, do not suffer these issues, and the stability at high speeds can be examined. The configuration that is considered is entered by first setting the translation speed to $c = 0.9$ and misaligning the beam until the first critical misalignment is reached at $a = 0.00643$. At this point the beam buckles into an out-of-plane equilibrium configuration with further misalignment. Misalignment is increased until the stable out-of-plane equilibrium at point o ($a = 0.00745$) is reached in Fig. 9 of (Orloske et al., 2005). From this configuration, speed is increased from $c = 0.9$ with fixed misalignment. Fig. 13 illustrates how the eigenvalues of branch o in Fig. 15 of (Orloske et al., 2005) evolve with increasing speed. At section p, a pair of purely imaginary, complex conjugate

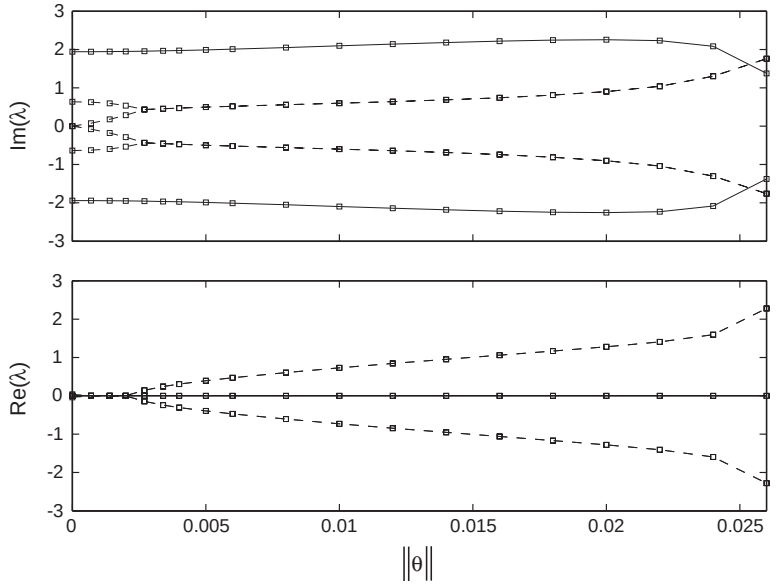

Fig. 12. Eigenvalues about the third out-of-plane solution branch in Fig. 9 of (Orloske et al., 2005) when $c = 0.9$. The dashed lines correspond to eigenvalues that cause instability.

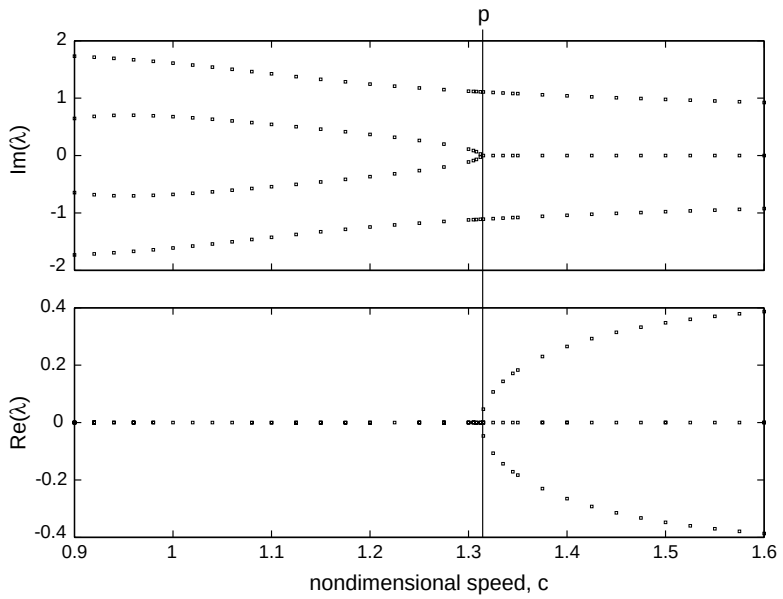

Fig. 13. Eigenvalues about branch o in Fig. 15 of (Orloske et al., 2005).

eigenvalues coalesce and divergence instability occurs. Therefore, like the trivial and planar equilibria, out-of-plane equilibria may also lose stability for sufficiently high translation speed.

4.3. Vibration modes

Because the axially moving beam system is gyroscopic, the eigenfunctions are complex, and the spatially varying phase angle of the eigenfunctions indicates the phase difference between points along the span. In this

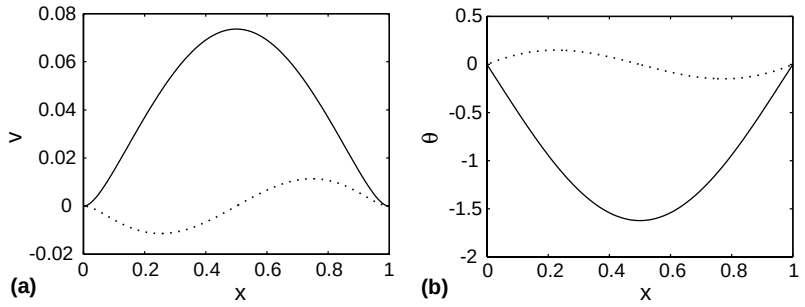

Fig. 14. Vibration modes about the aligned, trivial equilibrium when $c = 0.3$. The solid line is the real part and the dotted line is the imaginary part. (a) Lowest mode, $\omega = 3.15$. (b) Second lowest mode, $\omega = 5.59$.

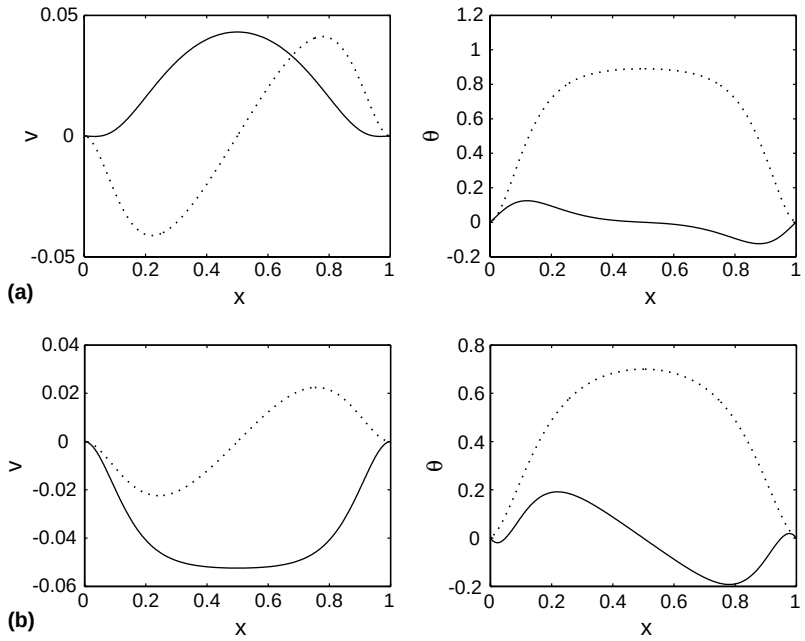

Fig. 15. Vibration modes about the planar equilibrium when $c = 0.3$ and $a = 0.01$. The solid line is the real part and the dotted line is the imaginary part. (a) Lowest mode, $\omega = 2.39$. (b) Second lowest mode, $\omega = 3.52$.

work, the magnitude of the discretized eigenfunctions $\widehat{\mathbf{Y}}$ are normalized such that $(\mathbf{M}\overline{\widehat{\mathbf{Y}}})^{\mathrm{T}}\widehat{\mathbf{Y}} = 1$ where the overbar denotes the complex conjugate.

Eqs. (10)–(13) are completely decoupled, so the vibration modes about the trivial equilibrium are also decoupled as illustrated in Fig. 14. When the equations of motion are linearized about a planar equilibrium solution, the planar deformation variables u and w decouple from the out-of-plane deformation variables v and θ. The vibration modes about the planar equilibria have only two components as shown in Fig. 15. The lowest frequency modes involve v and θ. When the equations of motion are linearized about an arbitrary equilibrium configuration, all deformation variables are coupled and the vibration modes about such an out-of-plane configuration contain all four deformation components. Examples are illustrated in Fig. 16. All vibration modes in Figs. 14–16 contain the symmetric and anti-symmetric properties typically found in stationary clamped–clamped beams.

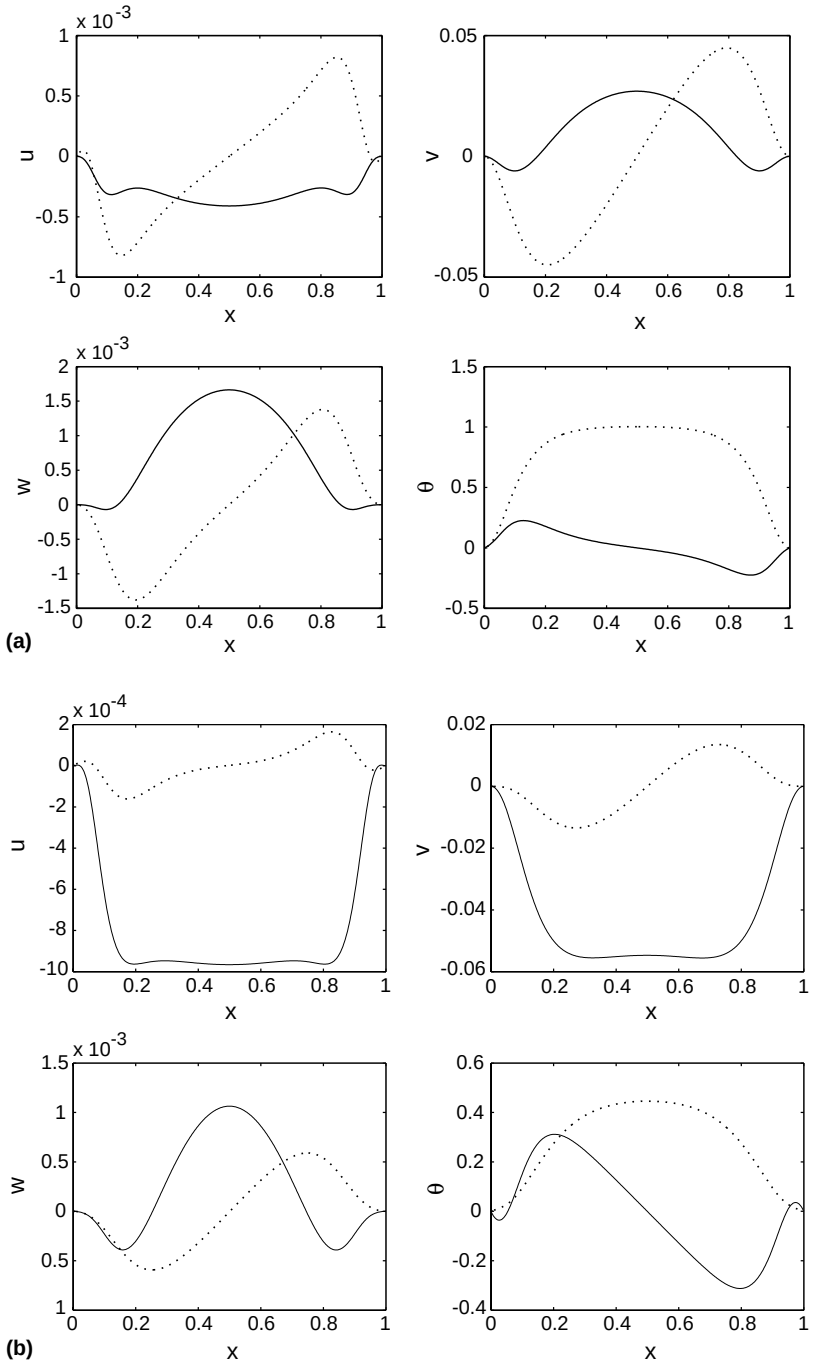

Fig. 16. Vibration modes about the out-of-plane equilibrium specified by point g in Fig. 9 of (Orloske et al., 2005). The solid line is the real part and the dotted line is the imaginary part. (a) Lowest mode, $\omega = 1.76$. (b) Second lowest mode, $\omega = 3.34$.

5. Conclusions

The nonlinear, three-dimensional, dynamic equations of motion for a misaligned translating beam are linearized about an arbitrary equilibrium configuration. The eigenvalue problem for vibration about an

equilibrium is discretized using finite difference approximations of the derivatives. Stability and vibration properties of the planar and non-planar equilibria include:

- The eigenvalues of the planar equilibria are strongly affected by changing speed. For the stationary beam, the stability of the planar equilibrium is lost after the first critical misalignment through divergence instability. A non-zero translation speed of $c = 0.3$ results in more complex eigenvalue behavior where both divergence and flutter instabilities exist. When speed is increased to $c = 0.9$ the eigenvalue behavior changes dramatically from the $c = 0.3$ case, and, under a specific range of misalignments, the planar equilibria regain stability after the first critical misalignment.
- At high speed ($c = 0.9$) more than one out-of-plane equilibrium configuration possesses stability. In contrast, at lower speed ($c = 0$ and $c = 0.3$) only the first bifurcated out-of-plane equilibrium is stable.
- When the equations of motion are linearized about a planar equilibrium solution, the planar deformation variables u and w decouple from the out-of-plane deformation variables v and θ. This causes the vibration modes about the planar equilibria to have only two components. In contrast, the vibration modes about out-of-plane equilibria possess all four components.

Appendix

The $\breve{G}_\alpha$ are, using the notation $\hat{u}, \hat{v}, \hat{w}, \hat{\theta}$ to denote u, v, w, and θ at an equilibrium solution,

$$\begin{aligned}\breve{G}_\alpha =& \frac{1}{2\mu\beta_\eta}\{[4(\Psi_{\alpha 1}\beta_\zeta + \Psi_{\alpha 2}j_\zeta - \Psi_{\alpha 3}j_\eta)\mu\sin^2\hat{\theta} + 8(\Psi_{\alpha 4}\beta_\zeta + (j_\zeta - j_\eta)\Psi_{\alpha 5})\mu\cos\hat{\theta}\sin\hat{\theta} \\ &+ 4(\Psi_{\alpha 6}\beta_\zeta + \Psi_{\alpha 7}j_\zeta - \Psi_{\alpha 8}j_\eta)\mu\cos^2\hat{\theta} + \Psi_{\alpha 9}]\beta_\eta \\ &+ (\Psi_{\alpha 10}\sin^2\hat{\theta} - 8\Psi_{\alpha 11}\cos\hat{\theta}\sin\hat{\theta} + \Psi_{\alpha 12}\cos^2\hat{\theta} + \Psi_{\alpha 13})\mu\beta_\zeta\}, \quad \alpha = u, v, w \\ \breve{G}_\theta =& [\Psi_{\theta 1}\beta_\zeta + (-2\Psi_{\theta 2}\sin^2\hat{\theta} - 8\Psi_{\theta 3}\cos\hat{\theta}\sin\hat{\theta} + 2\Psi_{\theta 4}\cos^2\hat{\theta})(j_\zeta - j_\eta)c + \Psi_{\theta 5}]\beta_\eta - 2\Psi_{\theta 6}\beta_\zeta\end{aligned} \tag{A.1}$$

where the $\Psi_{\alpha i}$ are

$$\begin{aligned}\Psi_{u1} =& -\left[\left(\theta\hat{w}'' + \frac{1}{2}v''\right)\hat{w}' + \left(-\theta\hat{v}'' + \frac{1}{2}w''\right)\hat{v}' + \frac{1}{2}w'\hat{v}'' + \frac{1}{2}v'\hat{w}''\right]\hat{\theta}' \\ &- \frac{1}{2}(\theta'\hat{v}'' + \theta\hat{v}''' - w''')\hat{w}' - \frac{1}{2}(\theta\hat{w}''' + \theta'\hat{w}'')\hat{v}' + \frac{1}{2}w'\hat{w}'''\end{aligned} \tag{A.2}$$

$$\begin{aligned}\Psi_{u2} =& -\left\{\left[\left(-\theta\hat{w}'' - \frac{1}{2}v''\right)\hat{w}' + \left(\theta\hat{v}'' - \frac{1}{2}w''\right)\hat{v}' - \frac{1}{2}w'\hat{v}'' - \frac{1}{2}v'\hat{w}''\right]\hat{\theta}'\right. \\ &\left. + \frac{1}{2}(-\theta'\hat{v}'' - \theta\hat{v}''' + w''')\hat{w}' + \frac{1}{2}(-\theta\hat{w}''' - \theta'\hat{w}'')\hat{v}' + \frac{1}{2}w'\hat{w}'''\right\}c^2 \\ &- \left[\frac{1}{2}(-\dot{v}'\hat{w}' - \dot{w}'\hat{v}')\hat{\theta}' + \left(-\frac{1}{2}\hat{v}''\dot{\theta} + \dot{w}''\right)\hat{w}' - \frac{1}{2}\dot{\theta}\hat{v}'\hat{w}''\right]c - \frac{1}{2}\ddot{w}'\hat{w}'\end{aligned} \tag{A.3}$$

$$\begin{aligned}\Psi_{u3} =& -\left\{\left[\left(-\theta\hat{w}'' - \frac{1}{2}v''\right)\hat{w}' + \left(\theta\hat{v}'' - \frac{1}{2}w''\right)\hat{v}' - \frac{1}{2}w'\hat{v}'' - \frac{1}{2}v'\hat{w}''\right]\hat{\theta}'\right. \\ &\left. + \frac{1}{2}(-\theta'\hat{v}'' - \theta\hat{v}''')\hat{w}' + \frac{1}{2}(-\theta\hat{w}''' - v''' - \theta'\hat{w}'')\hat{v}' - \frac{1}{2}v'\hat{v}'''\right\}c^2 \\ &- \left[\left(-\frac{1}{2}\dot{v}'\hat{w}' - \frac{1}{2}\dot{w}'\hat{v}'\right)\hat{\theta}' - \frac{1}{2}\dot{\theta}\hat{w}'\hat{v}'' - \frac{1}{2}\hat{v}'(\hat{w}''\dot{\theta} + 2\dot{v}'')\right]c + \frac{1}{2}\ddot{v}'\hat{v}'\end{aligned} \tag{A.4}$$

$$\begin{aligned}\Psi_{u4} =& \left[\left(-\theta\hat{v}'' + \frac{1}{2}w''\right)\hat{w}' + \left(-\theta\hat{w}'' - \frac{1}{2}v''\right)\hat{v}' - \frac{1}{2}v'\hat{v}'' + \frac{1}{2}w'\hat{w}''\right]\hat{\theta}' \\ &+ \frac{1}{2}(\theta'\hat{w}'' + \theta\hat{w}''' + \frac{1}{2}v''')\hat{w}' + \frac{1}{2}\left(-\theta\hat{v}''' - \theta'\hat{v}'' + \frac{1}{2}w'''\right)\hat{v}' + \frac{1}{4}v'\hat{w}''' + \frac{1}{4}w'\hat{v}'''\end{aligned} \tag{A.5}$$

$$\Psi_{u5} = \left\{ \left[\left(\theta\hat{v}'' - \frac{1}{2}w'' \right)\hat{w}' + \left(\theta\hat{w}'' + \frac{1}{2}v'' \right)\hat{v}' + \frac{1}{2}v'\hat{v}'' - \frac{1}{2}w'\hat{w}'' \right]\hat{\theta}' \right.$$
$$\left. + \frac{1}{2}(-\theta'\hat{w}'' - \theta\hat{w}''' - \frac{1}{2}v''')\hat{w}' + \frac{1}{2}\left(\theta\hat{v}''' + \theta'\hat{v}'' - \frac{1}{2}w''' \right)\hat{v}' - \frac{1}{4}v'\hat{w}''' - \frac{1}{4}w'\hat{v}''' \right\} c^2$$
$$+ \left[\frac{1}{2}(-\dot{w}'\hat{w}' + \dot{v}'\hat{v}')\hat{\theta}' + \frac{1}{2}(-\dot{v}'' - \hat{w}''\dot{\theta})\hat{w}' + \frac{1}{2}(-\dot{w}'' + \hat{v}''\dot{\theta})\hat{v}' \right] c - \frac{1}{4}\ddot{v}'\hat{w}' - \frac{1}{4}\ddot{w}'\hat{v}' \tag{A.6}$$

$$\Psi_{u6} = \left[\left(\theta\hat{w}'' + \frac{1}{2}v'' \right)\hat{w}' + \left(-\theta\hat{v}'' + \frac{1}{2}w'' \right)\hat{v}' + \frac{1}{2}w'\hat{v}'' + \frac{1}{2}v'\hat{w}'' \right]\hat{\theta}'$$
$$+ \frac{1}{2}(\theta'\hat{v}'' + \theta\hat{v}''')\hat{w}' + \frac{1}{2}(\theta\hat{w}''' + v''' + \theta'\hat{w}'')\hat{v}' + \frac{1}{2}v'\hat{v}''' \tag{A.7}$$

$$\Psi_{u7} = \left\{ \left[\left(-\theta\hat{w}'' - \frac{1}{2}v'' \right)\hat{w}' + \left(\theta\hat{v}'' - \frac{1}{2}w'' \right)\hat{v}' - \frac{1}{2}w'\hat{v}'' - \frac{1}{2}v'\hat{w}'' \right]\hat{\theta}' \right.$$
$$\left. + \frac{1}{2}(-\theta'\hat{v}'' - \theta\hat{v}''')\hat{w}' + \frac{1}{2}(-\theta\hat{w}''' - v''' - \theta'\hat{w}'')\hat{v}' - \frac{1}{2}v'\hat{v}''' \right\} c^2$$
$$+ \left[\frac{1}{2}(-\dot{v}'\hat{w}' - \dot{w}'\hat{v}')\hat{\theta}' - \frac{1}{2}\dot{\theta}\hat{w}'\hat{v}'' - \frac{1}{2}(\hat{w}''\dot{\theta} + 2\dot{v}'')\hat{v}' \right] c - \frac{1}{2}\ddot{v}'\hat{v}' \tag{A.8}$$

$$\Psi_{u8} = \left\{ \left[\left(-\theta\hat{w}'' - \frac{1}{2}v'' \right)\hat{w}' + \left(\theta\hat{v}'' - \frac{1}{2}w'' \right)\hat{v}' - \frac{1}{2}w'\hat{v}'' - \frac{1}{2}v'\hat{w}'' \right]\hat{\theta}' \right.$$
$$\left. + \frac{1}{2}(-\theta'\hat{v}'' - \theta\hat{v}''' + w''')\hat{w}' + \frac{1}{2}(-\theta\hat{w}''' - \theta'\hat{w}'')\hat{v}' + \frac{1}{2}w'\hat{w}''' \right\} c^2$$
$$+ \left[\frac{1}{2}(-\dot{v}'\hat{w}' - \dot{w}'\hat{v}')\hat{\theta}' + \left(-\frac{1}{2}\hat{v}''\dot{\theta} + \dot{w}'' \right)\hat{w}' - \frac{1}{2}\dot{\theta}\hat{v}'\hat{w}'' \right] c + \frac{1}{2}\ddot{w}'\hat{w}' \tag{A.9}$$

$$\Psi_{u9} = -\mu\hat{\theta}'[(v'\hat{v}' + w'\hat{w}')\hat{\theta}' + \theta'(\hat{v}'^2 + \hat{w}'^2 - 2)]\beta_\xi + (-2w'\hat{w}' - 2c\dot{u} - 2u'c^2 - 2v'\hat{v}')\mu$$
$$- 3w'\hat{w}'^3 + (-3v'\hat{v}' - 2u')\hat{w}'^2 + [-3\hat{v}'^2w' + (2 - 4\hat{u}')w']\hat{w}' - 3v'\hat{v}'^3$$
$$- 2\hat{v}'^2u' + (2 - 4\hat{u}')v'\hat{v}' + 2u' \tag{A.10}$$

$$\Psi_{u10} = -2[(-v'' - 2\theta\hat{w}'')\hat{w}' + (-w'' + 2\theta\hat{v}'')\hat{v}' - w'\hat{v}'' - v'\hat{w}'']\hat{\theta}'$$
$$+ 2(\theta\hat{v}''' + \theta'\hat{v}'')\hat{w}' + 2(\theta\hat{w}''' + \theta'\hat{w}'' + v''')\hat{v}' + 2v'\hat{v}''' \tag{A.11}$$

$$\Psi_{u11} = -\left[\left(\theta\hat{v}'' - \frac{1}{2}w'' \right)\hat{w}' + \left(\theta\hat{w}'' + \frac{1}{2}v'' \right)\hat{v}' + \frac{1}{2}v'\hat{v}'' - \frac{1}{2}w'\hat{w}'' \right]\hat{\theta}'$$
$$+ \frac{1}{2}(\theta'\hat{w}'' + \theta\hat{w}''' + \frac{1}{2}v''')\hat{w}' - \frac{1}{2}\left(\theta\hat{v}''' + \theta'\hat{v}'' - \frac{1}{2}w''' \right)\hat{v}' + \frac{1}{4}v'\hat{w}''' + \frac{1}{4}w'\hat{v}''' \tag{A.12}$$

$$\Psi_{u12} = -2[(2\theta\hat{w}'' + v'')\hat{w}' + (w'' - 2\theta\hat{v}'')\hat{v}' + w'\hat{v}'' + v'\hat{w}'']\hat{\theta}'$$
$$- 2(\theta\hat{v}''' - w''' + \theta'\hat{v}'')\hat{w}' - 2(\theta\hat{w}''' + \theta'\hat{w}'')\hat{v}' + 2w'\hat{w}''' \tag{A.13}$$

$$\Psi_{u13} = -[(v'\hat{v}' + w'\hat{w}')\hat{\theta}' + \theta'(\hat{v}'^2 + \hat{w}'^2 - 2)]\hat{\theta}' \tag{A.14}$$

$$\Psi_{v1} = \left(-\theta\hat{v}'' + \frac{1}{2}w'' \right)\hat{\theta}' + \frac{1}{2}\theta'\hat{w}'' + \frac{1}{2}\theta\hat{w}''' \tag{A.15}$$

$$\Psi_{v2} = \left[\left(\theta\hat{v}'' - \frac{1}{2}w'' \right)\hat{\theta}' - \frac{1}{2}\theta'\hat{w}'' - \frac{1}{2}\theta\hat{w}''' \right] c^2 + \frac{1}{2}(-\hat{w}''\dot{\theta} - \dot{w}'\hat{\theta}')c \tag{A.16}$$

$$\Psi_{v3} = \left[\left(\theta\hat{v}'' - \frac{1}{2}w''\right)\hat{\theta}' - \frac{1}{2}v''' - \frac{1}{2}\theta\hat{w}''' - \frac{1}{2}\theta'\hat{w}''\right]c^2 + \left(-\frac{1}{2}\hat{w}''\dot{\theta} - \dot{v}'' - \frac{1}{2}\dot{w}'\hat{\theta}'\right)c - \frac{1}{2}\ddot{v}' \tag{A.17}$$

$$\Psi_{v4} = \left(\theta\hat{w}'' + \frac{1}{2}v''\right)\hat{\theta}' - \frac{1}{4}w''' + \frac{1}{2}\theta'\hat{v}'' + \frac{1}{2}\theta\hat{v}''' \tag{A.18}$$

$$\Psi_{v5} = -\left[\left(\theta\hat{w}'' + \frac{1}{2}v''\right)\hat{\theta}' - \frac{1}{4}w''' + \frac{1}{2}\theta'\hat{v}'' + \frac{1}{2}\theta\hat{v}'''\right]c^2 - \frac{1}{2}(\hat{v}''\dot{\theta} - \dot{w}'' + \dot{v}'\hat{\theta}')c + \frac{1}{4}\ddot{w}' \tag{A.19}$$

$$\Psi_{v6} = \left(\theta\hat{v}'' - \frac{1}{2}w''\right)\hat{\theta}' - \frac{1}{2}v''' - \frac{1}{2}\theta\hat{w}''' - \frac{1}{2}\theta'\hat{w}'' \tag{A.20}$$

$$\Psi_{v7} = -\left[\left(\theta\hat{v}'' - \frac{1}{2}w''\right)\hat{\theta}' - \frac{1}{2}v''' - \frac{1}{2}\theta\hat{w}''' - \frac{1}{2}\theta'\hat{w}''\right]c^2 + \left(\frac{1}{2}\hat{w}''\dot{\theta} + \dot{v}'' + \frac{1}{2}\dot{w}'\hat{\theta}'\right)c + \frac{1}{2}\ddot{v}' \tag{A.21}$$

$$\Psi_{v8} = -\left[\left(\theta\hat{v}'' - \frac{1}{2}w''\right)\hat{\theta}' - \frac{1}{2}\theta'\hat{w}'' - \frac{1}{2}\theta\hat{w}'''\right]c^2 + \frac{1}{2}(\hat{w}''\dot{\theta} + \dot{w}'\hat{\theta}')c \tag{A.22}$$

$$\Psi_{v9} = (2\hat{v}'\theta' + \hat{\theta}'v')\hat{\theta}'\beta_\zeta\mu + 2(v' - \dot{v}c - v'c^2)\mu + (2\hat{u}' + 3\hat{v}'^2 + \hat{w}'^2)v' + 2(u' + w'\hat{w}')\hat{v}' \tag{A.23}$$

$$\Psi_{v10} = 2(-w'' + 2\theta\hat{v}'')\hat{\theta}' - 2\theta\hat{w}''' - 2\theta'\hat{w}'' - 2v''' \tag{A.24}$$

$$\Psi_{v11} = \left(\theta\hat{w}'' + \frac{1}{2}v''\right)\hat{\theta}' - \frac{1}{4}w''' + \frac{1}{2}\theta'\hat{v}'' + \frac{1}{2}\theta\hat{v}''' \tag{A.25}$$

$$\Psi_{v12} = 2(w'' - 2\theta\hat{v}'')\hat{\theta}' + 2\theta\hat{w}''' + 2\theta'\hat{w}'' \tag{A.26}$$

$$\Psi_{v13} = 2\theta'\hat{\theta}'\hat{v}' + v'\hat{\theta}'^2 \tag{A.27}$$

$$\Psi_{w1} = \left(\theta\hat{w}'' + \frac{1}{2}v''\right)\hat{\theta}' - \frac{1}{2}w''' + \frac{1}{2}\theta'\hat{v}'' + \frac{1}{2}\theta\hat{v}''' \tag{A.28}$$

$$\Psi_{w2} = -\left[\left(\theta\hat{w}'' + \frac{1}{2}v''\right)\hat{\theta}' - \frac{1}{2}w''' + \frac{1}{2}\theta'\hat{v}'' + \frac{1}{2}\theta\hat{v}'''\right]c^2 - \left(\frac{1}{2}\hat{v}''\dot{\theta} + \frac{1}{2}\dot{v}'\hat{\theta}' - \dot{w}''\right)c + \frac{1}{2}\ddot{w}' \tag{A.29}$$

$$\Psi_{w3} = -\left[\left(\theta\hat{w}'' + \frac{1}{2}v''\right)\hat{\theta}' + \frac{1}{2}\theta\hat{v}''' + \frac{1}{2}\theta'\hat{v}''\right]c^2 - \frac{1}{2}(\dot{v}'\hat{\theta}' + \hat{v}''\dot{\theta})c \tag{A.30}$$

$$\Psi_{w4} = -\left(-\theta\hat{v}'' + \frac{1}{2}w''\right)\hat{\theta}' - \frac{1}{4}v''' - \frac{1}{2}\theta\hat{w}''' - \frac{1}{2}\theta'\hat{w}'' \tag{A.31}$$

$$\Psi_{w5} = -\left[\left(\theta\hat{v}'' - \frac{1}{2}w''\right)\hat{\theta}' - \frac{1}{4}v''' - \frac{1}{2}\theta\hat{w}''' - \frac{1}{2}\theta'\hat{w}''\right]c^2 + \frac{1}{2}(\hat{w}''\dot{\theta} + \dot{w}'\hat{\theta}' + \dot{v}'')c + \frac{1}{4}\ddot{v}' \tag{A.32}$$

$$\Psi_{w6} = \left(-\theta\hat{w}'' - \frac{1}{2}v''\right)\hat{\theta}' - \frac{1}{2}\theta\hat{v}''' - \frac{1}{2}\theta'\hat{v}'' \tag{A.33}$$

$$\Psi_{w7} = \left[\left(\theta\hat{w}'' + \frac{1}{2}v''\right)\hat{\theta}' + \frac{1}{2}\theta\hat{v}''' + \frac{1}{2}\theta'\hat{v}''\right]c^2 + \frac{1}{2}(\dot{v}'\hat{\theta}' + \hat{v}''\dot{\theta})c \tag{A.34}$$

$$\Psi_{w8} = \left[\left(\theta\hat{w}'' + \frac{1}{2}v''\right)\hat{\theta}' - \frac{1}{2}w''' + \frac{1}{2}\theta'\hat{v}'' + \frac{1}{2}\theta\hat{v}'''\right]c^2 + \left(\frac{1}{2}\hat{v}''\dot{\theta} + \frac{1}{2}\dot{v}'\hat{\theta}' - \dot{w}''\right)c - \frac{1}{2}\ddot{w}' \tag{A.35}$$

$$\Psi_{w9} = (w'\hat{\theta}' + 2\theta'\hat{w}')\hat{\theta}'\beta_\zeta\mu + 2(-w'c^2 + w' - \dot{w}c)\mu + (2\hat{u}' + \hat{v}'^2 + 3\hat{w}'^2)w' + 2(u' + v'\hat{v}')\hat{w}' \tag{A.36}$$

$$\Psi_{w10} = 2(-v'' - 2\theta\hat{w}'')\hat{\theta}' - 2\theta'\hat{v}'' - 2\theta\hat{v}''' \tag{A.37}$$

$$\Psi_{w11} = \left(\theta\hat{v}'' - \frac{1}{2}w''\right)\hat{\theta}' - \frac{1}{4}v''' - \frac{1}{2}\theta\hat{w}''' - \frac{1}{2}\theta'\hat{w}'' \tag{A.38}$$

$$\Psi_{w12} = 2(v'' + 2\theta\hat{w}'')\hat{\theta}' - 2w''' + 2\theta'\hat{v}'' + 2\theta\hat{v}''' \tag{A.39}$$

$$\Psi_{w13} = w'\hat{\theta}'^2 + 2\theta'\hat{\theta}'\hat{w}' \tag{A.40}$$

$$\Psi_{\theta 1} = 2(\hat{v}''w'' + v''\hat{w}'' + \theta\hat{w}''^2 - \theta\hat{v}''^2)\sin^2\hat{\theta} + 8\left[\left(\theta\hat{v}'' - \frac{1}{2}w''\right)\hat{w}'' + \frac{1}{2}v''\hat{v}''\right]\cos\hat{\theta}\sin\hat{\theta} + 2(\theta\hat{v}''^2 - v''\hat{w}'' - \hat{v}''w'' - \theta\hat{w}''^2)\cos^2\hat{\theta} + 2(\hat{w}'\theta' + \hat{\theta}'w')\hat{w}'' + 2(\hat{v}'\theta' + \hat{\theta}'v')\hat{v}'' + 2(u'' + \hat{v}'v'' + \hat{w}'w'')\hat{\theta}' + (2\mu + 2\hat{u}' + \hat{v}'^2 + \hat{w}'^2)\theta'' + 2\theta'\hat{u}'' + 2(u' + v'\hat{v}' + w'\hat{w}')\hat{\theta}'' \quad (A.41)$$

$$\Psi_{\theta 2} = (\hat{v}''w'' + v''\hat{w}'' + \theta\hat{w}''^2 - \theta\hat{v}''^2)c + \dot{w}'\hat{v}'' + \dot{v}'\hat{w}'' \quad (A.42)$$

$$\Psi_{\theta 3} = \left[\left(\theta\hat{v}'' - \frac{1}{2}w''\right)\hat{w}'' + \frac{1}{2}v''\hat{v}''\right]c + \frac{1}{2}\dot{v}'\hat{v}'' - \frac{1}{2}\dot{w}'\hat{w}'' \quad (A.43)$$

$$\Psi_{\theta 4} = (\hat{v}''w'' + v''\hat{w}'' + \theta\hat{w}''^2 - \theta\hat{v}''^2)c + \dot{w}'\hat{v}'' + \dot{v}'\hat{w}'' \quad (A.44)$$

$$\Psi_{\theta 5} = 2(-\theta''c^2 - 2\dot{\theta}'c - \ddot{\theta})j_{\xi} + 2\theta''\beta_{\xi} \quad (A.45)$$

$$\Psi_{\theta 6} = (\hat{v}''w'' + v''\hat{w}'' + \theta\hat{w}''^2 - \theta\hat{v}''^2)\sin^2\hat{\theta} + 4\left[\left(\theta\hat{v}'' - \frac{1}{2}w''\right)\hat{w}'' + \frac{1}{2}v''\hat{v}''\right]\cos\hat{\theta}\sin\hat{\theta} + (\theta\hat{v}''^2 - v''\hat{w}'' - \hat{v}''w'' - \theta\hat{w}''^2)\cos^2\hat{\theta} + (-\hat{w}'\theta' - \hat{\theta}'w')\hat{w}'' + (-\hat{v}'\theta' - \hat{\theta}'v')\hat{v}'' - (u'' + \hat{v}'v'' + \hat{w}'w'')\hat{\theta}' + \left(-\mu - \hat{u}' - \frac{1}{2}\hat{v}'^2 - \frac{1}{2}\hat{w}'^2\right)\theta'' - \theta'\hat{u}'' - (u' + v'\hat{v}' + w'\hat{w}')\hat{\theta}'' \quad (A.46)$$

References

Doedel, E.J., Champneys, A.R., et al., 1997. Auto 97: Continuation and Bifurcation Software for Ordinary Differential Equations (with Homcont).

Hwang, S.J., Perkins, N.C., 1992. Supercritical stability of an axially moving beam Part II: Vibration and stability analyses. Journal of Sound and Vibration 154 (3), 397–409.

Koenig, H.A., 1998. Modern Computational Methods. Taylor & Francis, Philadelphia.

Mote Jr., C.D., 1965. A study of band saw vibrations. Journal of The Franklin Institute 279 (6), 430–444.

Orloske, K.M., Leamy, M.J., Parker, R.G., 2005. Flexural–torsional buckling of misaligned axially moving beams, I. Three-dimensional modeling, equilibria, and bifurcations. International Journal of Solids and Structures, this issue, doi:10.1016/j.ijsolstr.2005.08.014.

Pellicano, F., Vestroni, F., 2000. Nonlinear dynamics and bifurcations of an axially moving beam. Journal of Vibration and Acoustics, 122.

Simpson, A., 1973. Transverse modes and frequencies of beams translating between fixed end supports. Journal Mechanical Engineering Science 15 (3), 159–164.

Wickert, J.A.., 1992. Non-linear vibration of a traveling tensioned beam. International Journal of Non-Linear Mechanics 27 (3), 503–517.

Wickert, J.A., Mote Jr., C.D., 1990. Classical vibration analysis of axially moving continua. Journal of Applied Mechanics 57, 738–744.